

# Effects on soil properties of future settlements in downtown Mexico City due to ground water extraction

E. Ovando-Shelley, M. P. Romo, N. Contreras and A. Giralt

*Instituto de Ingeniería, UNAM, México, D.F., México*

Received: January 22, 2001; accepted: October 2, 2001

## RESUMEN

Como resultado del hundimiento regional producido por el bombeo de agua desde los acuíferos relativamente someros que yacen bajo la ciudad de México, muchos edificios han sufrido asentamientos diferenciales de gran magnitud. La consolidación inducida por el bombeo también modifica las propiedades estáticas y dinámicas del subsuelo. En este artículo se dan expresiones aproximadas para cuantificar la evolución de las propiedades del suelo. También se presenta uno de los escenarios plausibles sobre la futura distribución de asentamientos en el Centro Histórico de la ciudad, el cual sugiere que el patrimonio arquitectónico de la misma está amenazado por estos asentamiento y podría perderse en las próximas décadas, cuando menos parcialmente. Los resultados de un número limitado pero significativo de análisis de respuesta sísmica realizados considerando la evolución de las propiedades del suelo indican que el peligro sísmico y la distribución de este peligro se modificarán en el futuro. Algunas partes de la ciudad, como su Centro Histórico y la Zona de Transición, serán más vulnerables a temblores con contenidos de frecuencia altos en las siguientes décadas.

**PALABRAS CLAVE:** Hundimiento regional, subsuelo, evolución de propiedades del suelo, respuesta sísmica.

## ABSTRACT

Water pumping from shallow aquifers under Mexico City causes large differential settlements. Consolidation modifies the mechanical properties of the subsoil, both static and dynamic. Approximate expressions to predict soil properties are proposed. A scenario for the distribution of settlements in downtown Mexico City suggests that the city's architectural heritage could be partly lost in a few decades. Seismic response analyses considering future soil properties show that seismic hazard distribution in the city will change. Some parts of the city including the downtown area and the Transition Zone, may become more vulnerable to high frequency earthquakes.

**KEY WORDS:** Mexico City, evolution of soil properties, regional subsidence, seismic response

## INTRODUCTION

Much of the soil under Mexico City consists of low-strength, highly compressible lacustrine clays. Engineers have had to deal with these conditions since the XIVth century, when the city was founded by the Aztecs. Archaeological remains show that differential settlements affected pre-Hispanic structures such as massive earthen, stone-clad pyramids. Civil and religious buildings set up during Spanish rule also underwent large settlements which, in many cases, caused their destruction.

These problems were worsened by periodic floods especially at the beginning of the XVIIth century. Floodings were mitigated with a trench excavated in the mountains of the northern portion of the basin to divert one of the rivers that reached the lake. After its completion in the XVIIIth century, no further drainage works were undertaken until the late XIXth and the early XXth centuries. Drainage and land

reclamation for urban expansion produced the gradual shrinking of the lake, which is now practically nonexistent.

Regional subsidence was observed in the city even before pumping water from the aquifer that underlies the compressible clays began some 150 years ago. During the first half of the XXth century, pumping rates increased as did the city population. A relationship between population growth, amount of water extracted from the aquifer and subsidence rates was established by the pioneering work of Carrillo (1948), later continued by Marsal and Mazari (1959). Data collected by Tamez (1992) show that from 1900 to 1920 the settlement rate in downtown Mexico City was 3 cm/year; by the 1940's the rate was 13 cm/year and in the early 50's it reached 26 cm per year. Wells in downtown Mexico City were banned and settlement rates decreased to 5 cm/year. In the late 70's and early 80's new wells were put in operation in the outskirts, mainly near the hills that surround the city in the north and in the south. Settlement rates increased again

and in central Mexico City they now amount 7 to 10 cm/year but at some sites near the newer wells they exceed 30 cm/year (Mazari, 1996). The total subsidence over the last 100 years with respect to a reference point outside the lake zone now exceeds 8 m in some areas.

Surficial settlements are an expression of other internal, more complex changes that occur within the soil mass and modify its mechanical properties. The phenomenon depends on the amount and rate at which water is drawn from the aquifer. The rate of pumping has varied continuously over the years, as well as the number, location and distribution of water extraction points. Since variable pumping conditions are to be expected in the future, it is very difficult to make accurate predictions about changes in the geotechnical environment from information concerning the pumping operations. Nevertheless, some approximations can be made in order to estimate the magnitude of these changes in the future. We analyze and discuss some of the implications of these changes, especially future settlements in the older part of the city and possible modifications of the seismic response.

## GEOTECHNICAL ENVIRONMENT

Geotechnical conditions in Mexico City have been studied systematically since the 1950's (e. g., Marsal and Mazari, 1958). Geological processes present in the Basin of Mexico produced an ordered sequence of soft clay strata interspersed with lenses and layers of harder clayey silts with sands, in the larger part of the area occupied by the lakes.

*Surficial soils.* Much of downtown Mexico City rests on artificial fills, including the ruins of old pre-Hispanic buildings. These fills, rubble or masonry fragments in a remoulded clay matrix, can vary over short distances in the older part of the city where they sometimes reach depths of more than 15 m. In sites without artificial fills, a hard desiccated crust of low plasticity silt and silty or clayey fine sand, MH-ML, forms the upper stratum. It thins or may even be absent towards the east.

*Upper clay formation.* These are extremely compressible, highly plastic, volcanic clays interspersed with relatively thin lenses of volcanic ash or sandy silt. Water content in sites not subjected to surficial loads, mainly in the east, can sometimes be as high as 500 % whereas the clays found in the central part of the city, i. e. in sites subjected to large, permanent surface loads, contain pore water between 150 to 250 %. The clays can be as thick as 40 m in the centre of the lake and about 25 m in the old city core. Microfossils, diatomeas and other organic materials are frequently mixed with the clay, as well as small fragments of volcanic glass.

*First hard layer.* This is a sequence of seams and lenses of sands and sandy silts with clayey silts; softer silty clays are usually found between seams. Coarser material, even gravel, may be found towards the west, near the edge of the old lake bed, where its thickness can exceed 3 m and gets thinner toward the centre of the valley, where it may be absent or only be a few decimetres thick. Point-bearing piles usually rest on the first hard layer.

*Second clay formation.* These are also highly compressible clays that have been subjected to much larger overburdens and, consequently, are less compressible and display higher shear strengths than the upper formation. Thickness varies from about 2 to 5 m, and there are three or four thin layers of sands and sandy silts. The bottom is found at depths of about 55 m in the centre of the city and at more than 70 m toward the east side.

*Deep deposits.* These are alluvial deposits and older lacustrine clays that overlie the basalts, in the east, or the volcanic tuff, in the west, that constitute the basement.

For most practical purposes of foundation engineering or regional subsidence and seismic response, the relevant strata in this model reach down to the second clay formation. The same stratigraphical model is applicable to virtually anywhere in the lake zone, except for the edge of the old lake where the hard layers are thicker and more abundant and where the compressible clay strata are thinner. The distribution of strata along the margins of the old lake is also affected by the morphology of the mountain ranges that surround the lake and by the presence of alluvial fans from the hills in the west.

## CHANGES IN GEOTECHNICAL CONDITIONS

Exploitation of the aquifer reduced the pore water pressure within the clay masses. Pore pressures recorded under the National Palace with open head piezometers over the 1990-1999 period have been dropping steadily, as seen in Figure 1. These changes in pore pressure modify the mechanical properties of the clay masses which means that stress-path-stress-level dependent parameters like shear strength, compressibility and dynamic properties—shear moduli and damping factors—vary with time.

*Water content, volumetric weight and strength.* Figure 2 illustrates how water contents changed at a site in the Lake Zone. Data were taken from a sounding performed in 1952 (Marsal and Mazari, 1957) and from another one performed a couple of metres away, 34 years later, in 1986 (Jaime et al., 1987). Water content did not change significantly above 25 m; below this depth, the drop in water content can be attributed to consolidation in the clays propagating from the

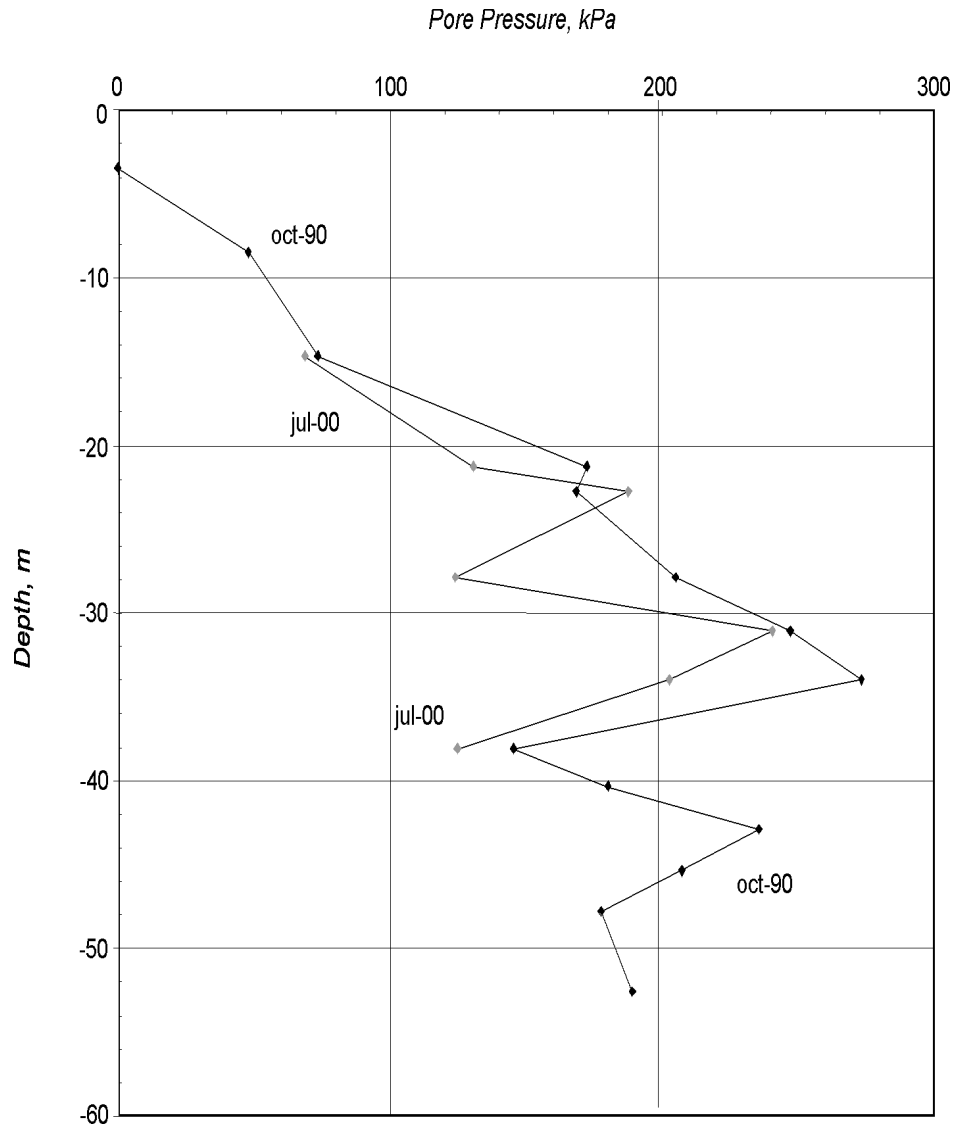


Fig. 1. Pore pressure distribution in 1990 and 2000 at a piezometric station in the National Palace in Mexico City.

deeper strata to the shallower ones. The figure also shows that the volumetric weight of the clays has increased by about 10 % on average; increments in strength are also evident. Similar variations have been found elsewhere in the city (Jaime and Romo, 1986).

*Compressibility.* Effective stress changes due to one dimensional loading of Mexico City clay are illustrated by the compressibility curves in Figure 3 (Méndez, 1991). These are the results of tests performed on two samples from the same stratum, one in 1952 and the other in 1986. Void ratio dropped from 7 to 5.8 between 1952 and 1986 whilst the apparent preconsolidation pressure increased from 72 to 85 kPa. The virgin consolidation line of the sample tested in 1986 matches the one obtained for the sample tested in 1952; thus, the general compressibility characteristics of the clay

were not affected by the regional subsidence. Since loading rate affects the shape of compressibility curves, care was taken to follow the same procedure.

#### EVOLUTION OF PORE PRESSURE AND AMOUNT OF SETTLEMENT

The consolidation process in the central part of Mexico City, as water is drawn from the underlying aquifers, can be studied using Terzaghi's consolidation theory. This provides reasonable estimates of delayed settlement in Mexico City (Carrillo, 1948; Marsal and Mazari, 1959). Other models have been used to study regional subsidence in the city, but this prospective study is adequately served by the Terzaghi model. We use Crank-Nicholson's implicit finite differences scheme

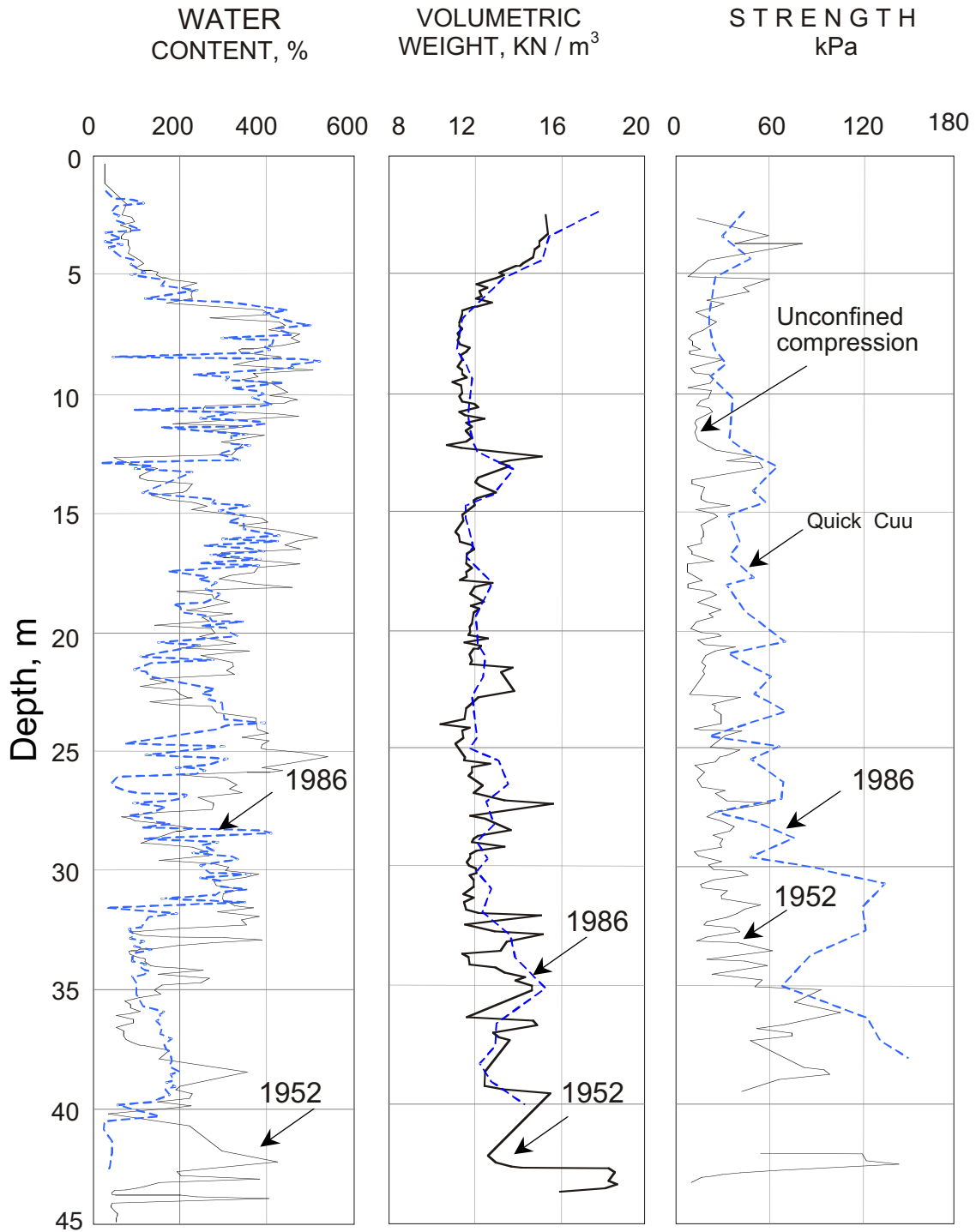


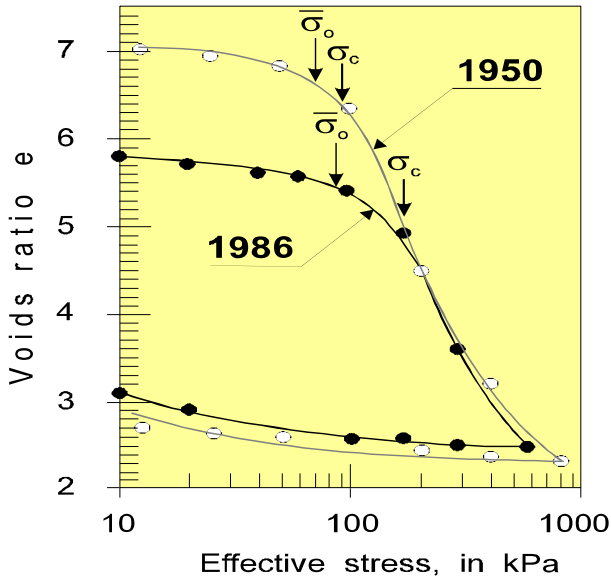
Fig. 2. Changes in water content, volumetric weight and strength at Río de Janeiro Square, Mexico City, during 1950-1986 (after Méndez, 1991).

(Isaacson and Keller, 1996) to incorporate time-dependent boundary conditions. Piezometric data from two sites in the centre of the city were used to calibrate the model.

The basic differential equation yields distributions of

excess pore pressure  $u$  with depth, for different time intervals in terms of the coefficient of consolidation  $c_v$ :

$$c_v \frac{\partial^2 u}{\partial z^2} = \frac{\partial u}{\partial t} \quad (1)$$



YEAR	Depth (m)	w <sub>i</sub> (%)	LL (%)	PL (%)	e <sub>i</sub>	S <sub>r</sub> (%)	σ̄' <sub>0</sub> kPa	σ' <sub>c</sub> kPa
1950	22.76	270	287	80	7.01	98	72	94
1986	21.87	262	290	85	5.82	102	85	160

Fig. 3. Compressibility curves of soil samples at Río de Janeiro Square, Mexico City, in 1950 and 1986 (after Méndez, 1991).

Initial and boundary conditions must be specified. The coefficient of consolidation depends on the volumetric compressibility  $m$ , and the permeability of the soil  $k$  as follows:

$$c_v = \frac{k}{m_v \gamma_w} \quad (2)$$

Permeability and compressibility are stress-level, stress-path dependent parameters but, for the purposes of a simplified model they were assumed to be constant.

*Evolution of pore pressure distribution in the clays.* The data from Figure 1 were reorganized to view time-varying pore pressures at different depths and at different times, over the 1990-2000 period (Figure 4). Pore pressure decay rate varied over a relatively narrow range, from 0.002 to 0.014 kPa/year. In the hard layer, between 38.0 and 40.0 m deep, pore pressure varied at a noticeably faster rate, as at the base of the second clay formation (47.8 m deep). Variations in head loss rates can be attributed to differences in the draining capacity of these lenses, which is much larger in the hard layer and in the deep deposits. Thus, a reasonable simplification is to model the old lake bed in Mexico City by two clay deposits. The upper boundary of the first layer is the water table and the lower, the first hard layer; the boundaries of the lower clay formation are the hard layer and the deep

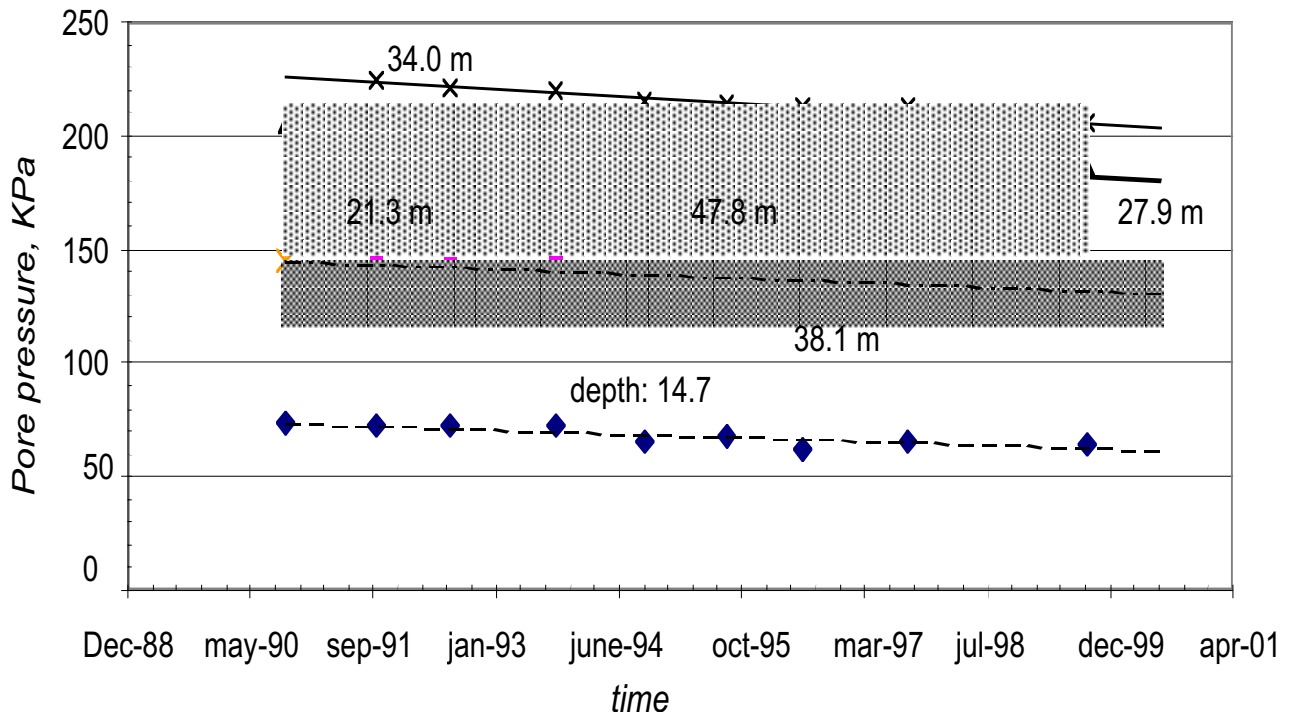


Fig. 4. Evolution of pore pressure at different depths under the National Palace from 1990 to 2000.

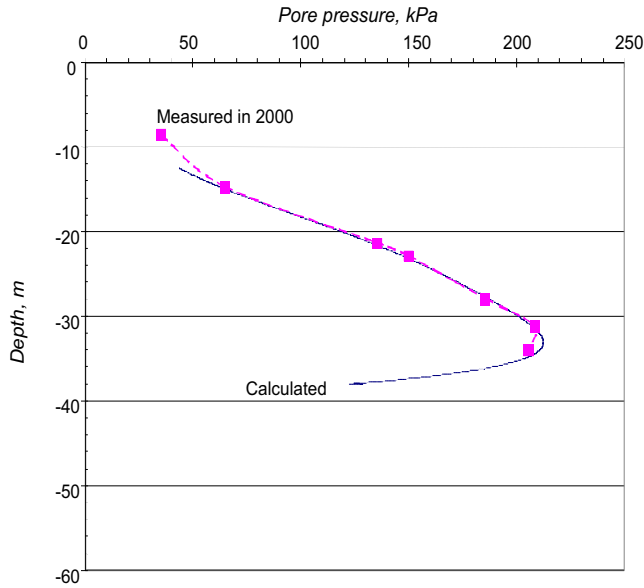


Fig. 5. Pore pressures in the Upper Clay Formation in 2000, compared with computed pore pressures, using initial conditions from data obtained in 1990 and time-varying boundary conditions from Figure 4.

deposits. This model does not include other compressible strata that underlie the two main clay formations.

Open head piezometers in Mexico City are usually installed in sandy lenses between clayey materials, so the pore pressure distributions shown in Figure 1 are approximations to those in the clays. However, recent pore pressure measurements in the clay layers performed with a piezocone suggest that the actual distributions of pore pressure do not differ substantially from those given in Figure 3 (Santoyo and Ovando-Shelley, 2000).

*Initial and boundary conditions.* Initial conditions were specified from piezometric readings at the beginning of the study period

$$u(z, 0) = f_i(z), \quad (3)$$

where  $f_i(z)$  is a polynomial fitted to the values of pore pressure in 1990 with  $z$  being the vertical depth in m. The conditions at the upper and lower boundaries can also be expressed as polynomial functions of time:

$$\begin{aligned} u(0, t) &= g(0, t) \\ u(2H, t) &= g(2H, t), \end{aligned} \quad (4)$$

where  $2H$  is the thickness of a clay stratum.

In the National Palace site a sixth-order polynomial was used to specify  $f_i(z)$  and straight lines were used to define  $g(0, t)$  and  $g(2H, t)$ .

*Calibration of the model.* The model was calibrated using pore pressure readings taken at the National Palace. Initial conditions were defined from piezometric data obtained in March 1990, and the boundary conditions from equations (3) and (4). The coefficient of consolidation  $c_v$  was found by trial and error until the model could reproduce the pore pressure distributions measured in March, 2000. The graph in Figure 5 shows the values of pore pressure calculated for 2000, closely match the measured ones, using  $c_v$  values of 0.0028 and 0.002 m<sup>2</sup>/s for the upper and lower clay strata, respectively.

*Evolution of pore pressures.* The model was then used to predict values of pore pressure at the National Palace site in ten year intervals up to the year 2100. The calculations assume that the pore pressure depletion rates from Figure 4 will be maintained in the future. Estimated pore pressure distributions in Figure 6 predict substantial reductions of pore pressure in the clay layers in the decades to come. Negative pore pressures at the boundaries represent an extreme condition in which flow of water occurs under non saturated conditions. A cut-off value of  $-1$  atm was introduced into the computer programme as a limiting value for pore pressure. Following the same procedure, future pore pressure distributions were also calculated for a site near the Metropolitan Cathedral. Results are qualitatively the same as those found for the National Palace site, as seen in Figure 7.

*Calculation of subsidence.* Pore pressure distributions as shown in Figures 6 and 7 can be used to obtain effective stress changes and to calculate settlements in the future. If one-dimensional compression is assumed, the following expression can be applied:

$$\delta(t) = \sum m_{vi} \Delta u_i(t) h_i, \quad (5)$$

where  $\Delta u_i(t)$  is the mean value of pore pressure decrements after the initial reference year, 1990, in a layer of soil of thickness  $h_i$ . Volumetric compressibilities were obtained from an empirical correlation that, as in Figure 8, relates them to cone penetration resistance  $q_c$ . Using Critical State Theory, this correlation can be expressed mathematically by means of an exponential function (Wroth, 1984; Wood, 1990; Tamez et al, 1997):

$$m_v = \alpha - \beta (\ln q_c) \quad (6)$$

where  $\alpha$  and  $\beta$  are stress-dependent constants:

$$\begin{aligned} \alpha &= 0.44 \text{ and } \beta = 0.13, \text{ for } q_c < 1600 \text{ kPa} \\ \alpha &= 0.253 \text{ and } \beta = 0.06, \text{ for } 1600 < q_c < 2600 \text{ kPa} \\ \alpha &= 0.13 \text{ and } \beta = 0.02, \text{ for } q_c > 2600 \text{ kPa.} \end{aligned} \quad (7)$$

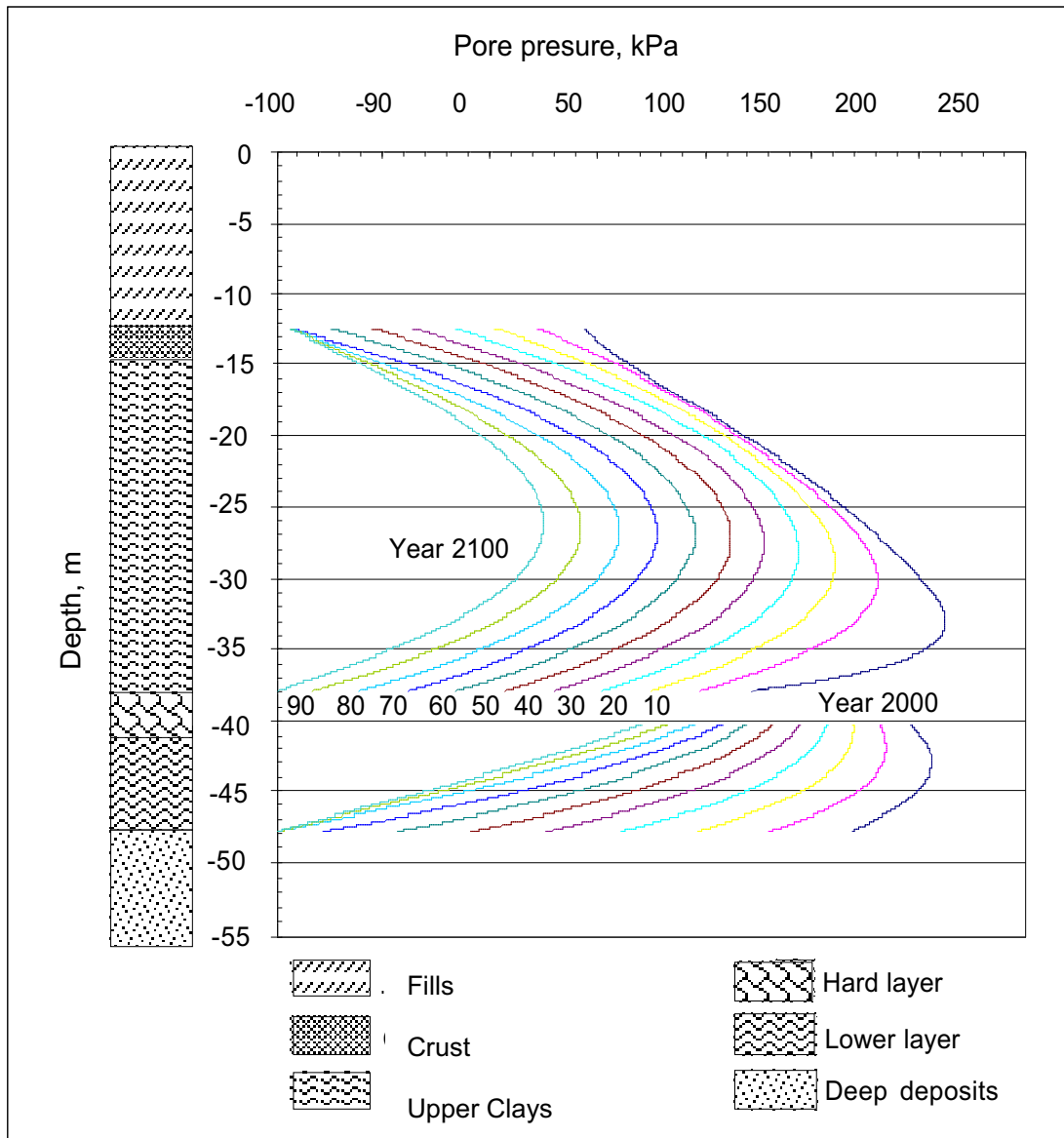


Fig. 6. Predicted pore pressure distribution at the National Palace, 1990 to 2100.

Since  $q_c$  is directly proportional to shear strength and the ratio between shear strength and vertical effective strength is constant for normally consolidated clays (Mexico City clay is normally consolidated or, at the most, lightly overconsolidated), changes in point penetration resistance and compressibility due to effective stress increments can be accounted for by (Santoyo *et al.*, 1989)

$$q_c = N_\sigma \sigma'_v(t) = N_\sigma (\sigma'_{v0} + \Delta u(t)), \quad (8)$$

where  $N_\sigma$  is a correlation coefficient equal to 5.5 and  $\sigma'_{v0}$  is the initial vertical effective stress. Even though this correlation shows some dispersion, it reflects a qualitatively correct trend.

Expressions (5) to (8) were used to estimate future settlement at the Cathedral site from two geotechnical soundings performed in 1989 (Tamez *et al.*, 1995). One of the soundings was performed in a place previously loaded by pre-Hispanic structures whilst at the other no such structures existed. Therefore,  $q_c$  values in the first site are larger than at the last sounding. Initial values of compressibility were estimated for every layer by averaging the  $q_c$  values from these two profiles using equation (6). Settlements were calculated at 10 year intervals by updating  $q_c$  and  $m_v$  with equations (8) and (6), and using the effective stress increments  $\Delta u(t)$  estimated from Figure 7. Table 1 gives the calculated settlements. The predicted total compression of the two clay strata is more than 2.4 m for the year 2100.

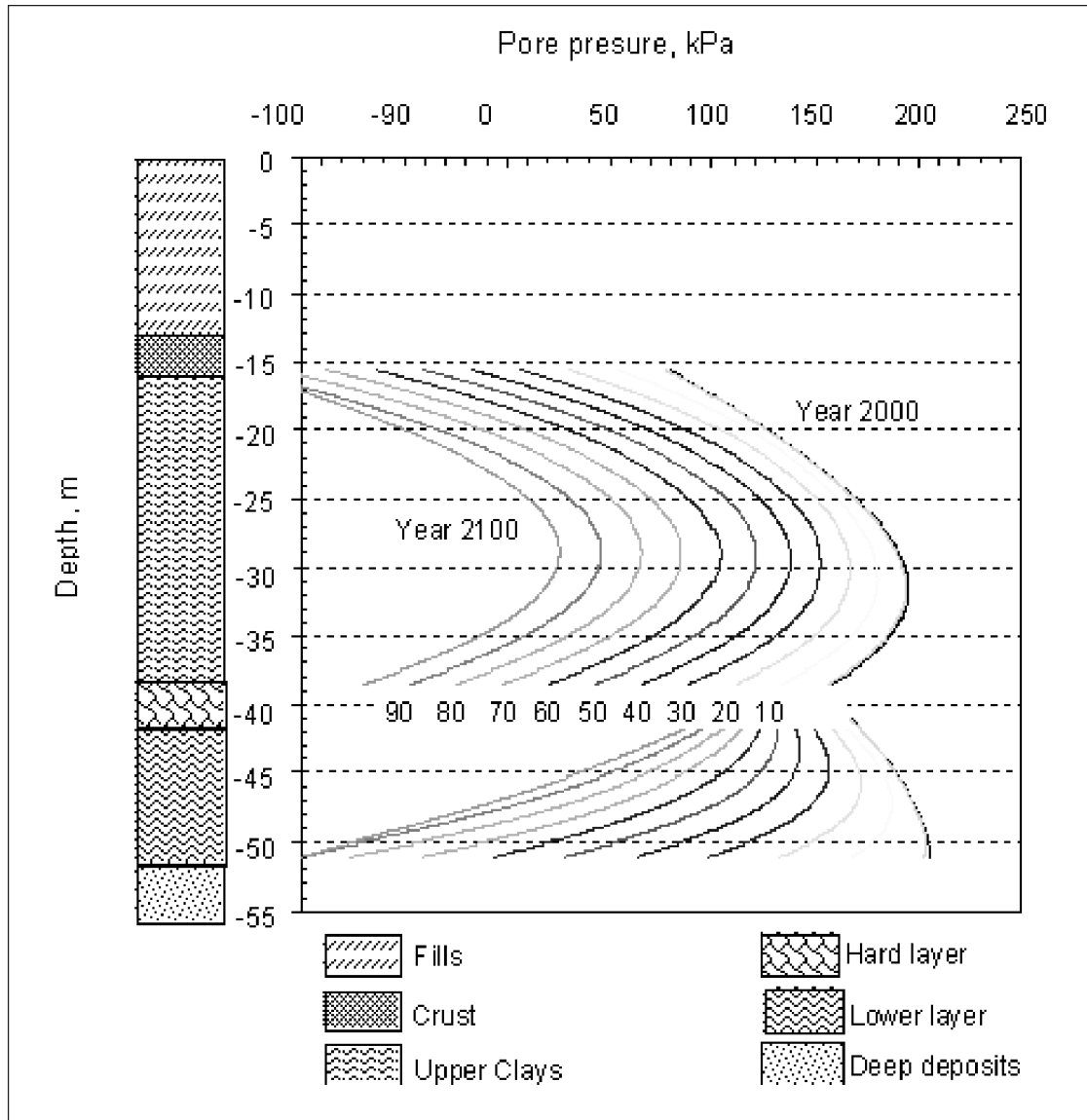


Fig. 7. Predicted pore pressure distribution at the Metropolitan Cathedral, 1990 to 2100.

Since the soils underlying the lacustrine clays settle additionally because of exploitation of the aquifer, the settlement calculated above is a lower bound of the expected total settlement at the site. From earlier deep benchmark readings, the contribution to the subsidence of the two clay strata used in this analysis is 69% (Tamez *et al.*, 1997). Hence the total settlement by the year 2100 could well exceed 3 m. This settlement must be added to the present value which was nearly 8.0 m from 1907 to 1989. These settlements are not uniform, as they depend on site dependent compressibility, which varies over central Mexico City.

Subsidence was predicted at 20 other sites. In these calculations initial compressibility values were obtained from CPT soundings and it was assumed that pore pressures would

evolve as in Figure 7. Figure shows 9 settlement contours estimated for the year 2075. From this scenario it is clear that many of the structures may not be able to sustain the differential settlements that will accumulate in the future unless major works are undertaken.

### EVOLUTION OF SOIL PROPERTIES

Changes in average water content, strength and compressibility can be estimated from approximate expressions of the dependency of these parameters on time. Dynamic shear moduli can be approximated with simplified formulae or from correlations with other geotechnical parameters.



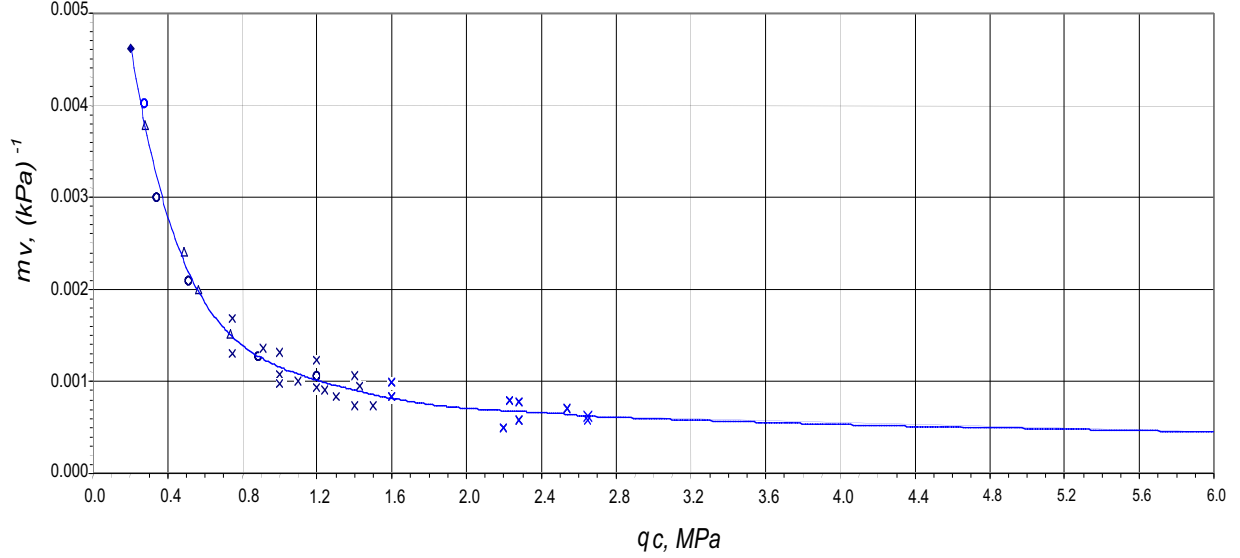


Fig. 8. Volumetric compressibility as a function of point penetration resistance from CPT tests (after Tamez *et al.*, 1995).

### Static properties

If compression in the clays is one dimensional, the following equations can be used to calculate the changes in water content from the amount of compression in the clay strata (Mazari *et al.*, 1985):

$$w_f = w_i \left[ 1 - \frac{\delta(t)}{H_T} \left[ \frac{1 + e_i}{e_i} \right] \right], \quad (9)$$

where  $w_i$  and  $w_f$  are the initial and final water content values of a clay layer of initial thickness  $H_T$ ;  $\delta(t)$  is the compression suffered by this layer and  $e_i$  is its initial void ratio. If full saturation of the clay is assumed,

$$w_f = w_i \left[ 1 - \frac{\delta(t)}{H_T} \left( 1 + \frac{1}{w_i G_s} \right) \right], \quad (10)$$

where  $G_s$  is the specific gravity.

Changes in bulk unit weights will be given by

$$\gamma_f = \frac{\gamma_i}{1 - \delta(t)/h_i}, \quad (11)$$

Shear strength can be explicitly written (Romo and Ovando-Shelley, 1989)

$$c_u(t) = \frac{M}{2} [p'_0 + \Delta u(t)] \exp\left(\frac{\Gamma - N}{\lambda}\right), \quad (12)$$

where  $M = 6 \sin \phi' / (3 - \sin \phi')$ ;  $\Gamma$  and  $N$  are the ordinates in  $e p'$  space at a reference pressure corresponding to the critical state and virgin consolidation lines;  $p'_0$  is the initial mean effective stress, and  $\phi'$  the friction angle in terms of effective stress. The parameter  $\lambda$  is the isotropic compressibility and is related to  $m_v$

$$m_v = \frac{\lambda}{(1 + e) \sigma'_v} = \frac{\lambda}{(1 + e) [\sigma'_0 + \Delta u(t)]}. \quad (13)$$

In equations (12) and (13), shear strength depends on effective stress increments and increases exponentially as the soil becomes less compressible.

### Dynamic properties

The dynamic properties of Mexico City clay are also modified by consolidation due to deep well pumping. Cyclic triaxial and resonant column tests have shown that the small-strain dynamic shear modulus of Mexico City clay can be expressed as (Romo, 1995; Romo and Ovando-Shelley, 1996):

$$G_{max} = 122 p_a \left( \frac{1}{PI - I_r} \right)^{(PI - I_r)} \left( \frac{\sigma'_c}{p_a} \right)^{0.82}, \quad (14)$$

where  $\sigma'_c$  is the effective confining pressure and  $p_a$  is the atmospheric pressure;  $PI$  is the plasticity index and  $I_r$  is the consistency index ( $= [LL - w_n] / PI$ ;  $LL$  = liquid limit). It should be noted that this relationship is only valid for  $PI - I_r > 0$  (Romo,

**Table 1**

Initial 1990 static soil properties and pore pressures for subsidence calculations

	Depth (m)	$G_s$	w (%)	$\sigma'_v$ (KPa)	$h_{vi}$ (m)	$Du_{vt}$ [t] (kPa)	$\gamma$ (kN/m <sup>3</sup> )	$q_c$ (MPa)	$m_{vi}$ (kPa) <sup>-1</sup>
Artificial fill	0,00 - 3,50	---	---	---	---	---	---	---	---
Artificial fill	3,50 - 12,50	---	---	---	---	---	---	---	---
Surface hardpan	12,50 - 15,50	---	---	---	---	---	---	---	---
Clay 1	15,50 - 17,50	2.39	227.503	13.34	2.00	1.0155	12.235	0.7	0.0018
Clay 2	17,50 - 21,00	2.44	228.043	13.69	3.50	0.3443	12.371	0.8	0.0017
Clay 3	21,00 - 26,00	2.50	237.379	15.25	5.00	0.6796	12.418	0.8	0.0017
Clay 4	26,00 - 28,00	2.39	226.631	17.98	2.00	0.9751	11.786	1.0	0.0014
Clay 5	28,00 - 31,50	2.39	236.606	21.71	3.50	1.2076	11.997	1.2	0.0012
Clay 6	31,50 - 33,00	2.39	211.450	26.09	1.50	1.4197	12.292	1.4	0.0010
Clay 7	33,00 - 38,50	2.35	238.586	30.22	5.50	1.7155	12.394	1.7	0.0009
Hard layer	38,50 - 41,00	---	---	35.00	2.50	---	14.000	---	---
Clay 8	41,00 - 42,50	2.47	165.814	42.12	1.50	0.6168	12.765	2.3	0.0007
Clay 9	42,50 - 45,00	2.37	143.546	41.43	2.50	0.4271	13.064	2.3	0.0007
Clay 10	45,00 - 51,00	2.46	151.910	45.01	6.00	0.7409	12.859	2.5	0.0006
Deep layers	51 -	---	---	---	---	---	---	---	---

$q_c$  = point penetration resistance;  $m_v$  = volumetric compressibility coefficient;  $G_s$  = specific gravity; w = water content;  $\gamma$  = volumetric weight;  $\sigma'_v$  = vertical effective stress;  $h_{vi}$  = initial thickness of clay strata;  $Du(t)$  = pore pressure decrement at time  $t$ .

1995). Equation (14) can also be written in terms of time dependent effective stress changes:

$$G_{max} = 122p_a \left( \frac{1}{PI - I_r} \right)^{(PI - I_r)} \left( \frac{\sigma'_c + \Delta u(t)}{p_a} \right)^{0.82} \quad (15)$$

Note that  $I_r$  in equations (14) and (15) will also change with time because of equation (9).

The dependency of shear modulus with strain has been expressed by hyperbolic functions (Romo, 1995; Romo and Ovando-Shelley, 1996):

$$G = G_{max} (1 - H(\gamma)) \quad (16)$$

where

$$H(\gamma) = \left[ \frac{(\gamma/\gamma_r)^{2B}}{1 + (\gamma/\gamma_r)^{2B}} \right]^A \quad (17)$$

$G$  is the shear modulus for a shear strain  $\gamma$  and  $\gamma_r$  is a reference shear strain, defined as the strain for a 50% drop in the shear modulus.  $A$  depends on an experimental function of plasticity index  $A'$  and on relative consistency, i. e.  $A = A' + I_r$ ;  $B$  is another experimental function. Plots of  $A'$  and  $B$  against plasticity index are given in Figures 10 and 11. As expected,  $\gamma$  also depends on plasticity index or relative consistency (Figure 12). The influence of plasticity index on the dynamic stiffness-strain behaviour of clays was noted previously (e.g. Dobry and Vucetic, 1987).

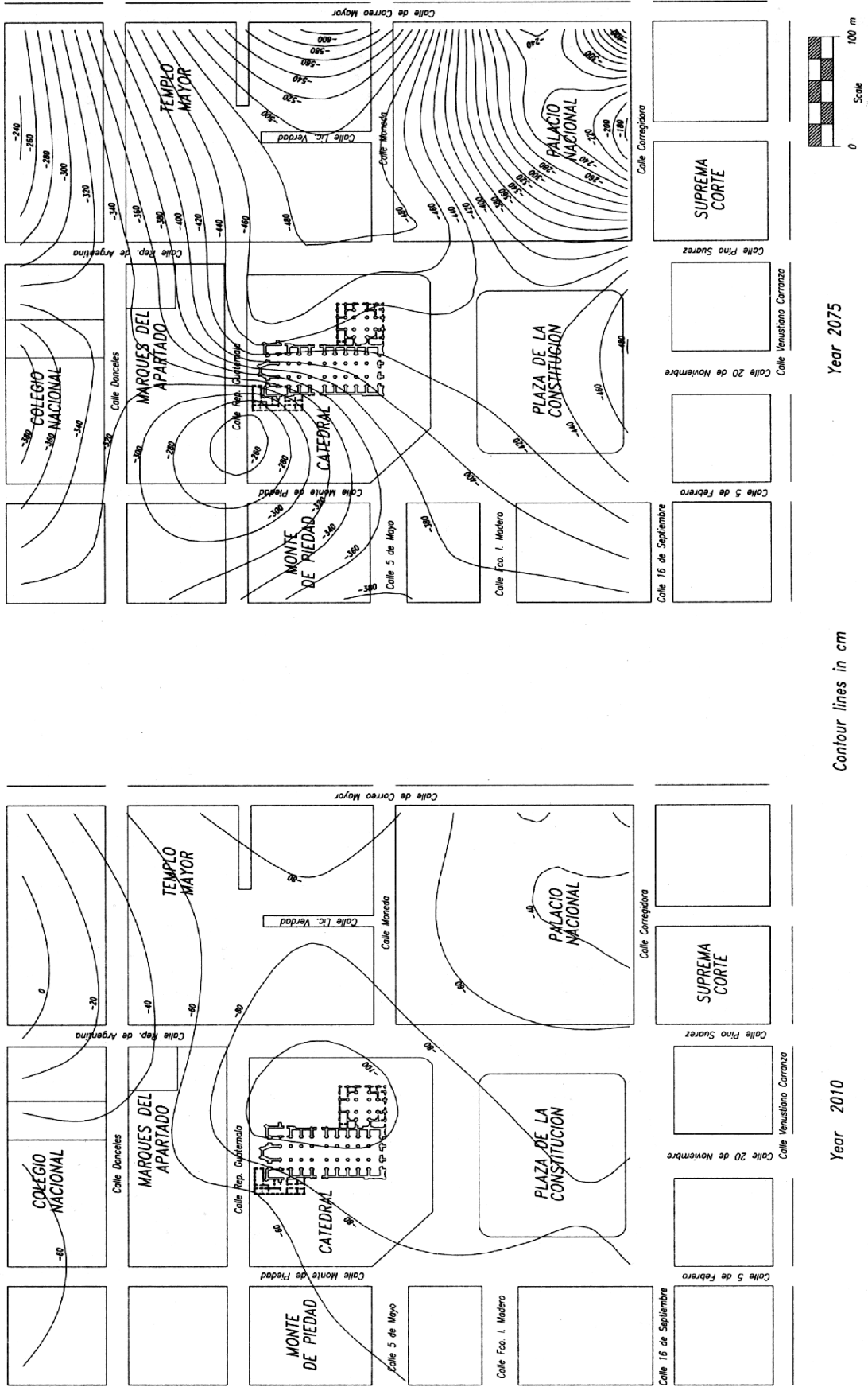


Fig. 9. Predicted settlements in central Mexico City for the years 2010 and 2075.

If the soil behaves like a viscoelastic material before failure, hysteretic damping coefficients may be expressed as

$$\lambda = (\lambda_{max} - \lambda_{min})H(\gamma) + \lambda_{min}, \quad (18)$$

where  $\lambda_{max}$  and  $\lambda_{min}$  are the maximum and minimum values of the damping coefficient, obtained experimentally for  $\gamma=10\%$  and  $\gamma=10^{-4}\%$  respectively.

$G_{max}$  is sometimes obtained indirectly from shear wave velocity measurements as

$$G = \rho V_s^2 = \frac{\gamma_{nat}}{g} V_s^2, \quad (19)$$

where  $V_s$  is the shear wave velocity,  $\rho$  the mass density,  $\gamma_{nat}$  the *in situ* volumetric weight and  $g$  the acceleration of gravity.

Using cavity expansion theory with a hyperbolic approximation to model the soil's nonlinear behaviour, Ovando-Shelley and Romo (1992) estimated shear wave velocity from point penetration resistance  $q_c$  measured from CPT tests performed in the lake zone of Mexico City:

$$V_s = \eta \sqrt{\frac{q_c}{\gamma_{nat} N_{kh}}}, \quad (20)$$

where  $\eta$  depends on soil type and  $N_{kh}$  is a correlation parameter. Values in equation (20) have been discussed for Mexico City clays (Ovando-Shelley and Romo, 1992). Shear wave velocities have been related to  $q_c$  using neural networks (Romo *et al.*, 2000) but expression (11) provides sufficiently accurate results for this study. In order to derive equation (20), results of CPT soundings were compared with down-hole, seismic cone and suspension-logging tests. Strains in these tests are small, typically  $10^{-4}\%$  or less. As shear moduli depend strongly on strain, the values of  $G$  from shear wave

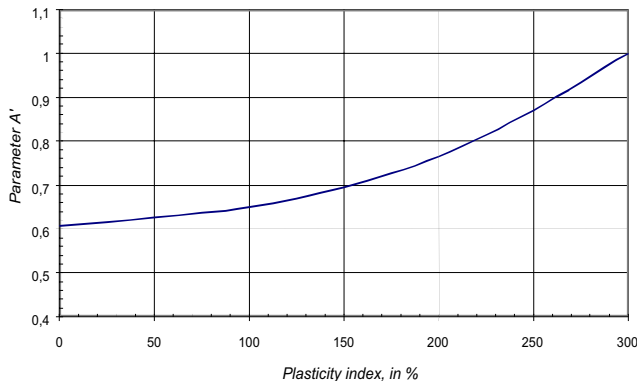


Fig. 10. Variation of parameter A' with plasticity index.

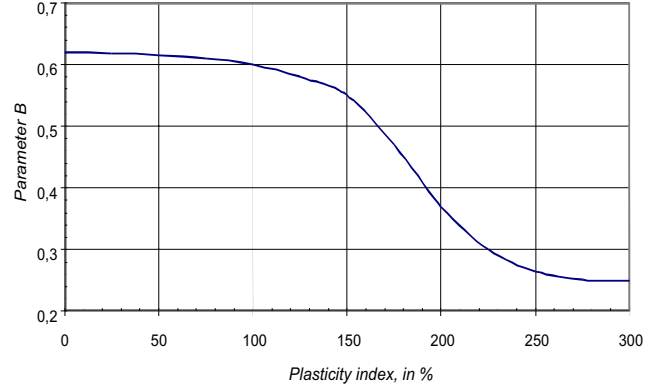


Fig. 11. Variation of parameter B with plasticity index.

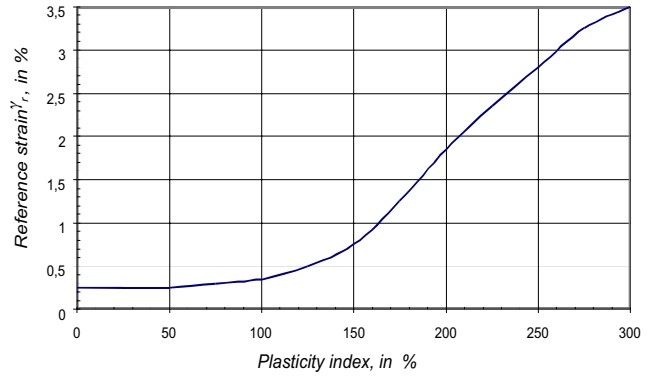


Fig. 12. Variation of the reference strain  $\gamma_r$  with plasticity index.

velocities *in situ* are close to the maximum values of the shear modulus,  $G_{max}$ .

Consolidation induced by pumping in Equation (20) can be estimated from Equations (8) and (11):

$$V_s = \eta \sqrt{\frac{q_c + N_\sigma \Delta u(t)}{\gamma_{nat} N_{kh}}} = \eta \sqrt{\frac{q_c + N_\sigma \Delta u(t)}{\left(\frac{\gamma_i}{1 - \delta(t)/h_i}\right) N_{kh}}}. \quad (21)$$

Introducing into Equation (19):

$$G_{max}(t) = \frac{\eta^2}{g} \left( \frac{q_{ci} + N_\sigma \Delta u_i(t)}{N_{kh}} \right). \quad (22)$$

The complete stiffness-strain curves can be approximated using Equation (16):

$$G_{max}(t) = \frac{\eta^2}{g} \left( \frac{q_{ci} + N_\sigma \Delta u_i(t)}{N_{kh}} \right) (1 - H(\gamma)). \quad (23)$$

Equations (6) to (15) will be affected by changes in pore pressures and effective stresses induced by the consolidation process taking place within the clay masses that underlie the lake zone of Mexico City.

Figure 13 shows the stiffness-strain and damping-strain curves from Equations (23) and (18). The values of  $\Delta u(t)$  were obtained from Figure 7 for a clay stratum under the Cathedral at a depth of 35.5 m. The shape of the curves is not affected noticeably by the increments in effective stress produced by regional pumping. On the contrary, initial stiffness increases sharply on account of pumping-induced consolidation. On the other hand, the curves in Figure 13 show that damping is not affected by changes in effective stress.

The dominant period at a site is a useful parameter in seismic response analysis. It is also affected by changes in material properties brought about by regional consolidation. Assuming elastic behaviour, dominant period may be expressed as

$$T_0 = \frac{4(h - \delta(t))}{\sqrt{G_{avg} / \rho_{avg}}} = \frac{4(h - \delta(t))}{V_{savg}}, \quad (24)$$

where  $G_{avg}$ ,  $\rho_{avg}$ , and  $V_{savg}$  are the average values of the shear modulus, the density and the shear wave velocity, respectively. In a stratified medium the average velocity may be approximated by

$$V_{savg} = \frac{4(h - \delta(t))}{\frac{\sum V_{si} h_i(t)}{\sum h_i(t)}}. \quad (25)$$

#### CHANGE IN SEISMIC RESPONSE OF A SITE IN DOWNTOWN MEXICO CITY

Seismic response analyses using a one dimensional model for vertically propagating waves have been used to predict the seismic response of Mexico City clay deposits in the old lake zone (Rosenblueth, 1952; Romo, 1995; Rosenblueth and Ovando-Shelley, 1995). The model used in this research is one dimensional and solves the equations of motion using the Haskell-Thomson approach solution for a stratified medium (Haskell, 1953; Thomson, 1950). The computer programme finds the response of the soil column using random vibration theory, given in terms of power spectral densities and using extreme value theory (Bárcena and Romo, 1994). The programme calculates maximum accelerations, strains, mean maximum stresses and response spectra at different depths. Soil strata are assumed to be viscoelastic materials characterized by

frequency-independent, nonlinear, stiffness-strain and damping-strain curves such as in equations (14) to (18). If material nonlinearities need to be introduced, the programme makes use of the linear equivalent method.

Average soil properties were taken from Tamez *et al* (1995). The surficial fills, the upper clay formation, the hard layer and the lower clay formation, were divided into 16 substrata, down to a depth of 51 m. Initial values of the relevant parameters are shown in Table 2. Shear wave velocities and initial shear moduli were calculated, as well as the stiffness-strain and damping-strain curves corresponding to each layer. Changes in volumetric weights, point penetration resistance, and in the thicknesses of the layers were obtained using the pore pressures calculated previously for different times in the future. Input motions at the base of the model from response spectra were obtained for accelerograms at a basalt outcrop in the south of the city, which is equivalent to assuming rigid materials underlying the soils below 51 m.

Figures 14 and 15 show response spectra obtained from response spectra at the National University for the 11 January, 1997 earthquake ( $M_c = 7.1$ ). Nonlinear soil properties were introduced in some analyses and introduced noticeable but relatively small changes in the spectral ordinates and in the dominant period. The figures also show response spectra obtained for an accelerometric station at the Cathedral's west atrium. These spectra do not show the sharp peaks present in the the calculations. Response from actual accelerations in the site are influenced by the vicinity of the Cathedral, a very massive structure. Thus, the Cathedral interacts strongly with the soil during earthquakes, especially along the east-west direction as indicated in Figure 14, which is related to rocking about the Cathedral's longitudinal axis whereas movements along the north-south direction are mainly shearing modes. The model yielded good approximations to the dominant period and to the spectral ordinates at the site.

The evolution of the site's seismic response is examined using input motions from two other earthquakes. The great Michoacán earthquake of 19 September, 1985 that originated along the subduction zone off the Mexican Pacific coast, 300 km from the city ( $M_c = 8.1$ ). Motions produced by subduction quakes contain low frequency components which are amplified by the soft Mexico City clays. The Tehuacán earthquake of 15 June, 1999, was located 186 km south-east of the city ( $M_c = 7.1$ ). Normal faulting earthquakes like the latter contain more higher-frequency components.

Response spectra at the National University during the great Michoacán earthquake of 1985 show that the dominant period may drop substantially in the future (Figure 16). If the dominant period shortens due to stiffening of the clays,

maximum spectral amplitudes may increase steadily. With the soil properties as obtained in 2000, the maximum spectral acceleration turned out to be about 0.65 g whereas the value estimated for the year 2100 reached 1.15 g. Maximum ground acceleration may also increase substantially: from 0.14 g for 2000 to 0.3 in the year 2100. However, spectral amplification –i.e. the ratio between spectral ordinates and maximum ground acceleration– may still vary over a relatively narrow range at the site natural period: between 4.0 and 4.8, as in Figure 17. Interestingly, the spectral ordinates

for the second mode had a relatively small amplitude, over the next 100 years. Spectral amplification below 0.4 s was insignificant. Even for very large spectral ordinates, the material would remain within the linear range, as shown in Figure 18, which shows the evolution of the dominant period, with and without nonlinear stress-strain and damping-strain curves.

Future spectral response to the Tehuacán earthquake also shows the effect of the sharp reduction in natural pe-

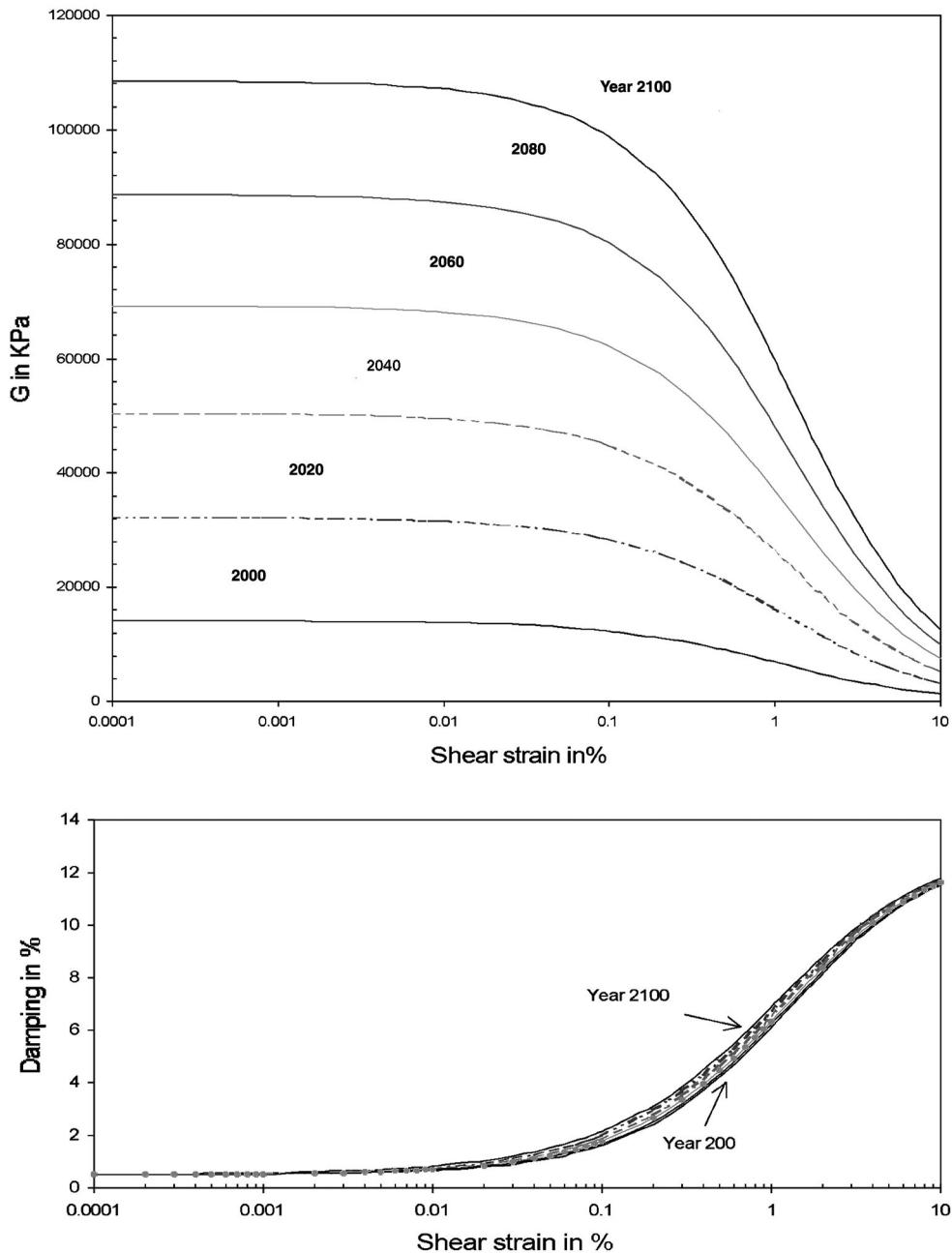


Fig. 13. Changes in shear modulus  $G$  and damping  $\lambda$  in a soil stratum located under the Cathedral’s southern atrium at a depth of 36 m.

**Table 2**

Initial (1990) conditions and soil properties for seismic response analysis

	Depth (m)	$q_c$ (MPa)	$h$ (m)	$\gamma$ (kN/m <sup>3</sup> )	$V_s$ (m/s)	$G_{max}$ (MPa)	$\lambda$
Artificial fill	0,00 - 3,50	---	3.50	16.000	250.00	0.10204	0.06
Artificial fill	3,50 - 12,50	2.5	9.00	13.000	200.00	0.05306	0.05
Surface hardpan	12,50 - 15,50	7.5	3.00	14.000	180.00	0.04629	0.05
Clay 1	15,50 - 17,50	0.7	2.00	12.235	72.83	0.00613	0.03
Clay 2	17,50 - 21,00	0.8	3.50	12.371	75.43	0.00664	0.03
Clay 3	21,00 - 26,00	0.8	5.00	12.418	75.38	0.00666	0.03
Clay 4	26,00 - 28,00	1.0	2.00	11.786	86.54	0.00833	0.03
Clay 5	28,00 - 31,50	1.2	3.50	11.997	93.97	0.01000	0.03
Clay 6	31,50 - 33,00	1.4	1.50	12.292	100.27	0.01167	0.03
Clay 7	33,00 - 38,50	1.7	5.50	12.394	110.04	0.01417	0.03
Hard layer	38,50 - 41,00	6.50	2.50	14.000	395.83	0.12844	0.05
Clay 8	41,00 - 42,50	2.3	1.50	12.765	125.86	0.01908	0.03
Clay 9	42,50 - 45,00	2.3	2.50	13.064	124.39	0.01907	0.03
Clay 10	45,00 - 51,00	2.5	6.00	12.859	130.11	0.02054	0.03
Deep layers	51 -	---	---	16.400	1500.000	0.52421	0.07

$h(m)$  = layer thickness;  $q_c$  = point penetration resistance;  $\gamma$  = volumetric weight;  $G_{max}$  = initial (small strain) stiffness;  $\lambda$  = damping;  $V_s$  = shear wave velocity.

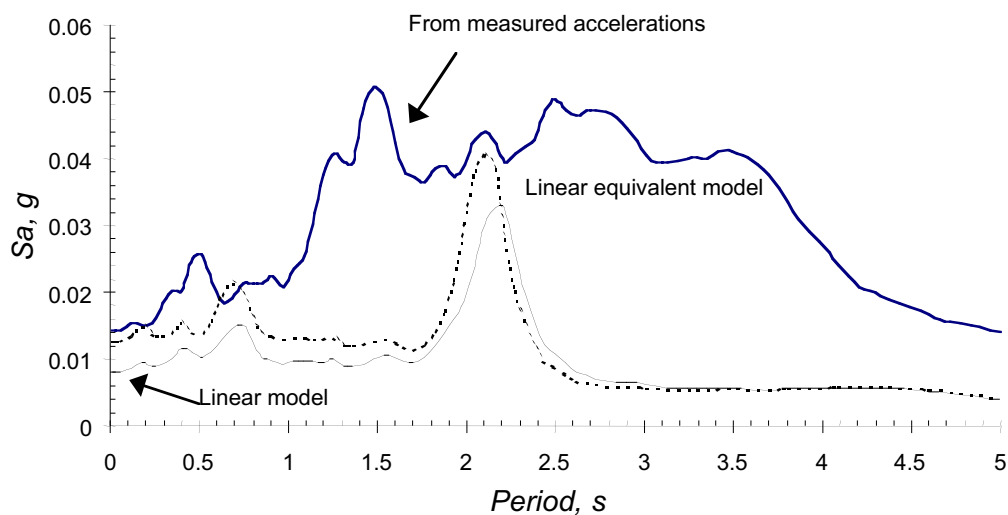


Fig. 14. Response spectra obtained from accelerations measured in the Cathedral’s atrium during the 11 January 1977 earthquake and accelerations calculated with the RADSH programme, with and without strain dependent non-linear soil properties (East-West component).

riod. Spectral ordinates increased steadily from 2000 to 2040; between 2040 to 2060, they remain basically constant and increase again in 2100 (Figure 19). Spectral ordinates for the second mode are more significant than for the 1985 event. Maximum ground accelerations vary from 0.014 g in the year 2000 to 0.05 g in 2100 and spectral ordinates at the first mode go from 0.036 g to 0.128 g. Spectral amplifications at the natural period could change from 2.2 to 3.2 and from 2.1 to 2.4 for the second mode (Figure 20). Nonlinear effects are negligible, as expected since ground motion in the Tehuacán event was smaller than for the Michoacán earthquake (Figure 21).

Other earthquakes also affect Mexico City but these two events represent extreme examples of the actual motions.

### CONCLUSIONS

Soil strata in the central part of Mexico City have suffered complex loading and unloading patterns due to the construction of pre-Hispanic, colonial and modern buildings. These loading histories modified the mechanical properties, mainly the strength and compressibility of the soil. Non-homogeneous geotechnical conditions prevail in central Mexico City. Buildings have undergone large differential settlements due to self weight consolidation. Exploitation of the aquifers under the lacustrine clays began about 150 years ago producing additional differential settlements in hundreds of structures built between the XVIth and the early XXth centuries. The soil in central Mexico City is still consolidating due to piezometric head losses produced by pumping and will continue to do so in the future. Damage to a large number of

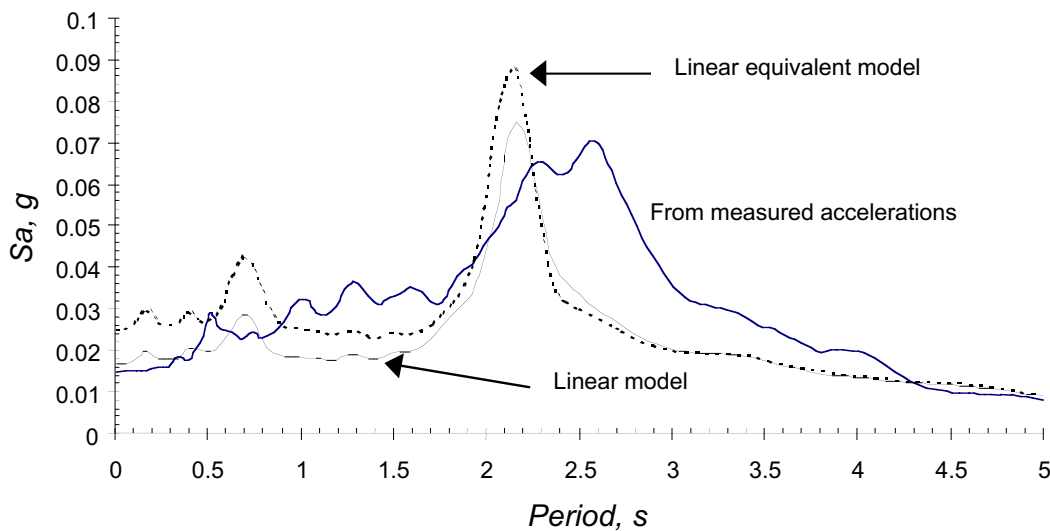


Fig. 15. As in Figure 14 (North-south component).

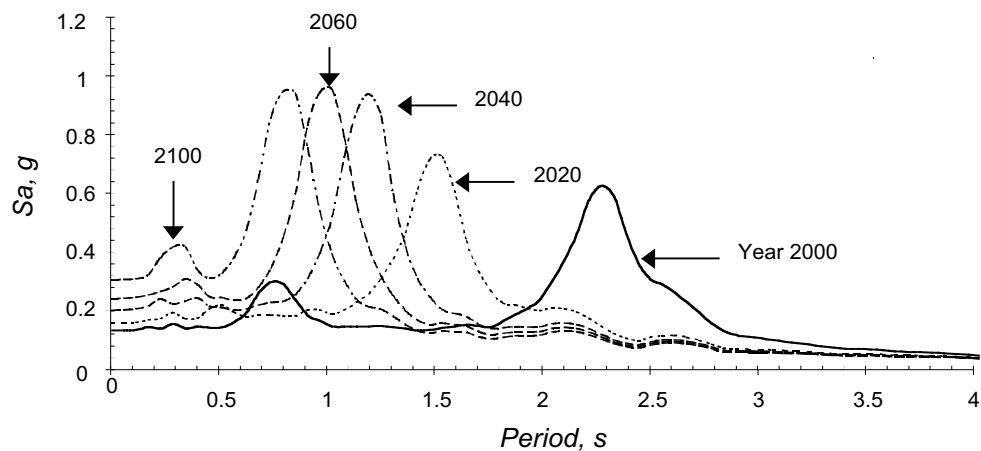


Fig. 16. Response spectra from 2000 to 2100. Input motions at the base of the soil column as recorded at a basalt outcrop during the 19 September 1985 earthquake (east-west acceleration).



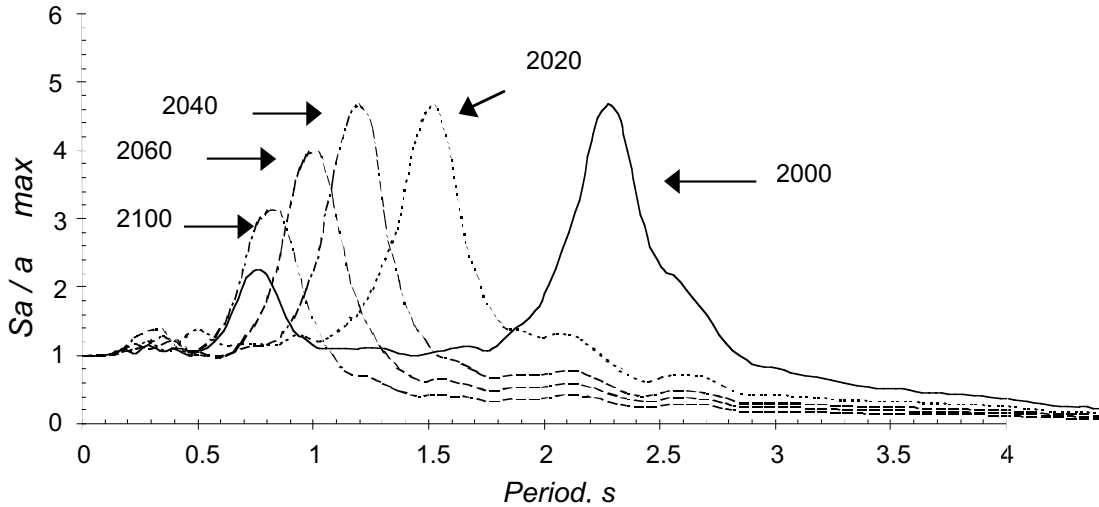


Fig. 17. Normalized response spectra for 2000-2100. Input motion as in the preceding figure.

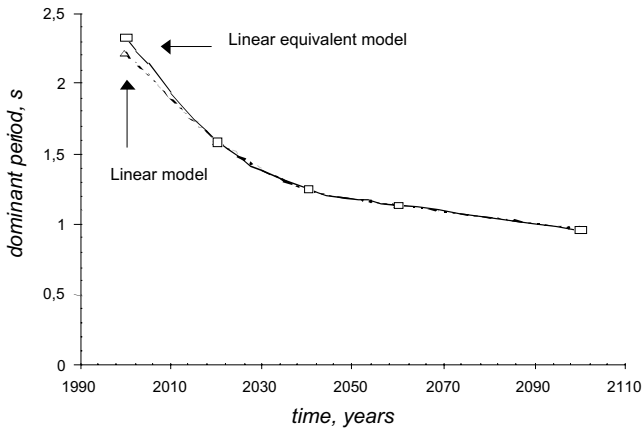


Fig. 18. Changes in the natural period at the Cathedral's atrium from the two preceding figures.

structures is to be expected, including much of the city's architectural heritage.

Surface settlements are but a part of other, more complex internal changes within these clays. We discuss the effects of regional subsidence on the static and dynamic properties of the clays in central Mexico City. Water content, density, strength and compressibility will change as pore pressures decrease due to the exploitation of the aquifer. These future changes can be estimated.

One-dimensional consolidation theory is useful to study the evolution of pore pressures in the future, using boundary conditions from piezometric data gathered over the last 10 years in the centre of the city. We predict that buildings will sustain large differential settlements in the years to come. These settlements plus the ones presently existing will very seriously endanger many structures, unless remedial meas-

ures are undertaken. The scenario in Figure 9 is by no means exact, yet it is plausible. It gives a qualitative view of the type and magnitude of the problems that should be dealt with in the future to prevent further damage to structures and to estimate the costs involved.

Dynamic soil properties will also change because of regional subsidence. Expressions for estimating changes in stiffness and damping as strain dependent variables, were given. The increase in effective stresses due to pumping is very significant in terms of stiffness, but negligible for damping.

A one-dimensional wave propagation model with strain-dependent nonlinearity was used to obtain response spectra at a site in central Mexico City. Drastic reductions in dominant period are to be expected in the next few decades. After about 60 years, stiffening of the clays will occur at a slower rate. Future seismic behaviour was examined for two earthquakes having different source mechanisms: the 19 September 1985 earthquake, a subduction event rich in long-period components and the 15 June 1999 Tehuacán earthquake where short period components were important. In general, seismic hazard will increase at the site, especially during large magnitude normal faulting earthquakes because of the gradual stiffening of the clays in the future.

Several general conclusions relevant for the seismic design of buildings in the city can be drawn from these results:

- a) Depletion of pore pressures within the clayey soils in Mexico City produces changes in soil properties, both static and dynamic, that cannot be ignored.

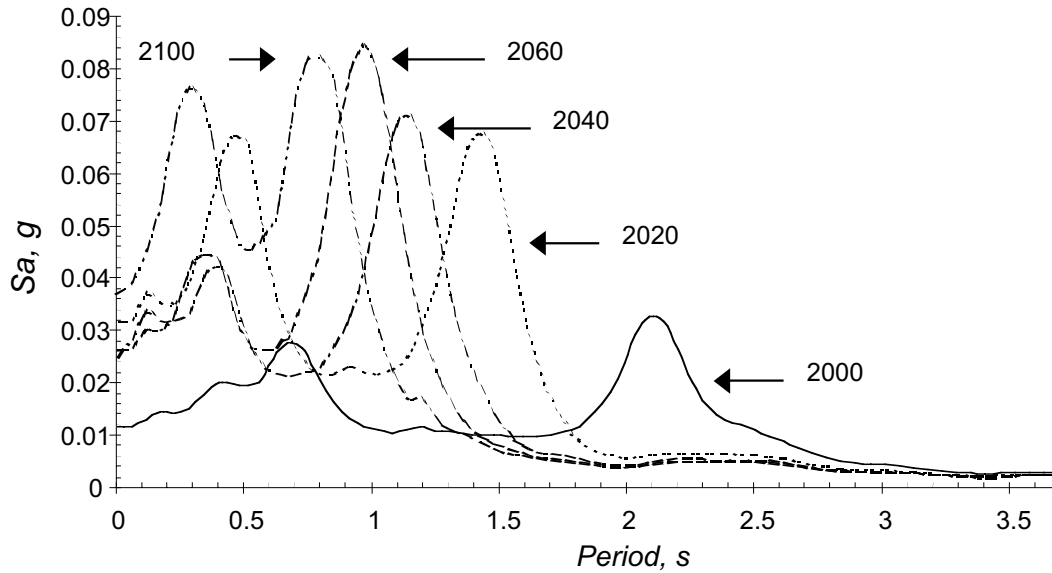


Fig. 19. Response spectra for the 2000-2100 period. Input motions at the base of the soil column as recorded at a basalt outcrop during the 19 September 1985 earthquake (north-south component).

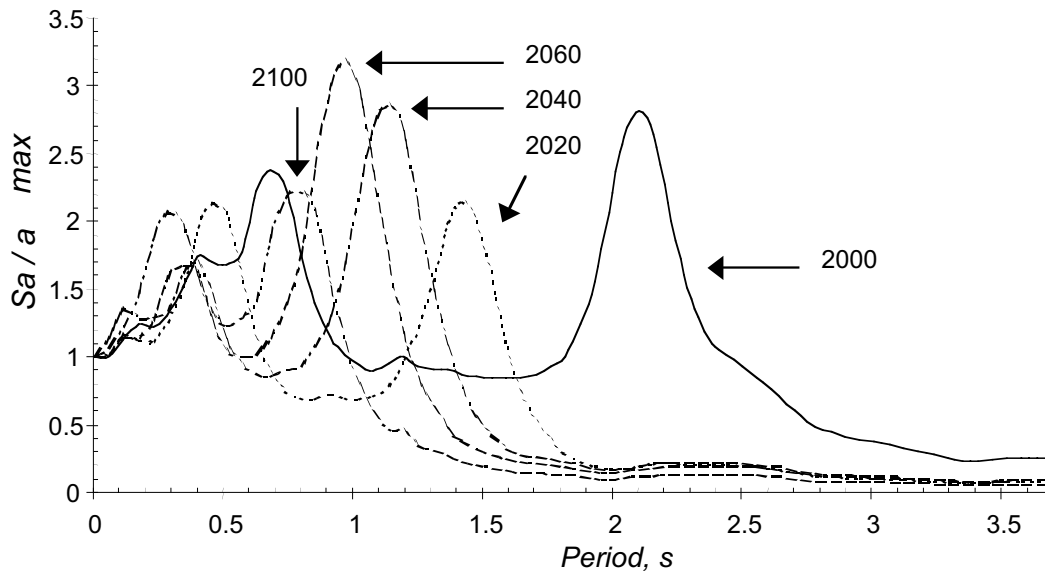


Fig. 20. Normalized response spectra for the 2000-2100. Input motion as in the preceding figure.

- b) Stiffening of the clay shortens the dominant period of the soil deposits, thus modifying existing iso-period maps in the building code.
- c) Changing soil properties will modify seismic hazard in the lake and transition zones and vulnerability of structures in this area.
- d) Overall shortening of dominant periods will change the zones in which seismic movements are more intense in the city.
- e) In the case of subduction earthquakes, the most hazardous zones will slowly migrate towards the centre of the old lake bed.
- f) The transition zone near the edge of the lake will become more vulnerable to high-frequency events such as deep normal faulting earthquakes or events produced by neighboring active faults (Acambay).
- g) Certain parts of central Mexico City, subjected to high, long standing external loads and to the effects of regional

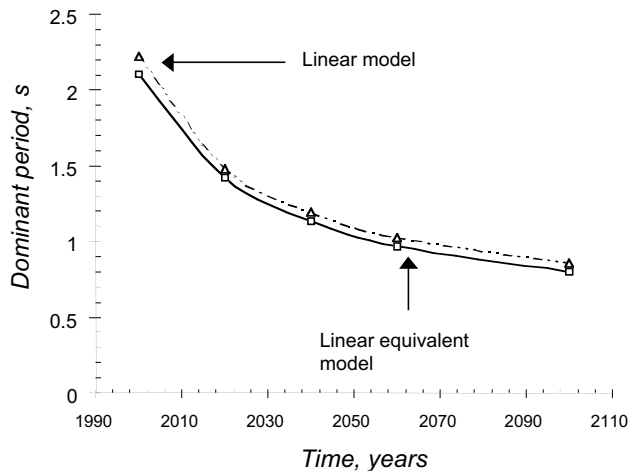


Fig. 21. Changes in the natural period at the Cathedral's atrium from the two preceding figures.

subsidence will become more vulnerable to high frequency events.

#### ACKNOWLEDGMENTS

The government of the Federal District, Mexico City, sponsored this investigation. The help of Sergio Zaldívar, Enrique Santoyo and Enrique Tamez is gratefully acknowledged.

#### BIBLIOGRAPHY

- BÁRCENA, A. and M. P. ROMO, 1994. RADSH: programa de computadora para analizar depósitos de suelo estratificados horizontalmente sujetos a excitaciones dinámicas aleatorias. Internal Report, México: Instituto de Ingeniería, UNAM.
- CARRILLO, N. 1948. Influence of artesian wells in the sinking of Mexico City, Proc. 2nd Int. Conf on Soil Mech. and Found. Engng., Rotterdam, v II.
- DOBRY, R. and M. VUCETIC, 1987. Dynamic properties and seismic response of soft clay deposits. Proc. Simposio Internacional de Ingeniería Geotécnica de Suelos Blandos, M. J. Mendoza (editor), México, Sociedad Mexicana de Mecánica de Suelos, 2, 49-85.
- HASKELL, N. H., 1953. The dispersion of surface waves in multilayered media. *Bull. Seism. Soc. Am.*, 43, 17-34.
- ISAACSON, E. and H. B., KELLER, 1996. Analysis of numerical methods. New York: John Wiley & Sons.

- JAIME, A. and M. P., ROMO, 1986. Características del suelo en el sitio Plaza Río de Janeiro. Internal Report, Mexico City, Instituto de Ingeniería, UNAM.
- MARSAL, R. J. and M. MAZARI, 1969. The subsoil of Mexico City, Mexico: School of Engineering, UNAM.
- MAZARI, M., R. J., MARSAL and J. ALBERRO, 1985. The settlements of the Aztec great temple analysed by Soil Mechanics. Mexico: Mexican Society for Soil Mechanics.
- MAZARI, M., 1996. La isla de los perros, Mexico: El Colegio Nacional.
- MÉNDEZ, E., 1991. Evolución de las propiedades de la arcilla de la ciudad de México. B Sc. Thesis, México, Escuela Superior de Ingeniería y Arquitectura, Instituto Politécnico Nacional.
- OVANDO-SHELLEY, E. and M. P. ROMO, 1992. Estimación de la velocidad de propagación de ondas S en la arcilla de la ciudad de México. *Sismodinámica*, 2, 107-123.
- ROMO M. P. and E. OVANDO-SHELLEY, 1989. Effective shear strength from undrained tests, Serie Gris, Pub. No. E-59, Mexico: Instituto de Ingeniería, UNAM.
- ROMO, M. P., 1995. Clay behaviour, ground response and soil-structure interaction studies in Mexico City. State of the Art Paper. Proc. Third Int. Conference on Recent Advances in Geotechnical Engineering and Soil Dynamics, S. PRAKASH (editor), University of Missouri, Rolla, Saint Louis, Missouri.
- ROMO, M. P. and E. OVANDO-SHELLEY, 1996. Modeling the dynamic behaviour of Mexican clays, Proc. XII Int Conf. on Earthq. Engn., Acapulco, Mexico, CD edition.
- ROSENBLUETH, E., 1952. Teoría del diseño sísmico sobre mantos blandos. Ediciones ICA, México, Serie B 14, 3-12.
- ROSENBLUETH, E. and E. OVANDO-SHELLEY, 1995. Geotechnical lessons from Mexico City and other recent earthquakes. Proc. Second Int. Conference on Recent Advances in Geotechnical Engineering and Soil Dynamics. S. Prakash (editor), University of Missouri, Rolla, Saint Louis, Missouri, Vol. 2, 1799-1811.
- SANTOYO, E., R. LIN and E. OVANDO-SHELLEY, 1989. El cono en la exploración geotécnica. México: TGC Geotecnia.

SANTOYO, E. and E. OVANDO-SHELLEY, 2000. Catedral y Sagrario de la ciudad de México: Corrección geométrica y endurecimiento del subsuelo. Technical report submitted to the Mexican Council for Culture and Art (CONACULTA).

TAMEZ, E., 1992. Differential settlements in colonial buildings in Mexico City's historical centre, XI Nabor Carrillo Lecture, Mexico: Mexican Society for Soil Mechanics.

TAMEZ, E., E. SANTOYO, A., CUEVAS and E. OVANDO-SHELLEY, 1995. Diagnóstico y proyecto geotécnico. Chapter II. *In*: Catedral Metropolitana: corrección geométrica, informe técnico. Mexico City: Asociación de Amigos de la Catedral Metropolitana de México, A. C., S. Zaldívar (editor), 41–114.

TAMEZ, E., E. OVANDO-SHELLEY and E. SANTOYO, 1997. Underexcavation of the Metropolitan Cathedral in Mexico City. Proc. XIVth International Conference on Soil Mechanics and Foundation Engineering, Special Invited Lecture, Hamburg, 4, 2105-2126.

THOMSON, W. T., 1950. Transmission of elastic waves through a stratified soil. *J. Appl. Phys.*, 21, 89-93.

---

E. Ovando-Shelley, M. P. Romo, N. Contreras and A. Giralt

*Instituto de Ingeniería, UNAM, AP 70-472, Coyoacán 04510, Mexico, D. F. México*

*Email. eovs@pumas.iingen.unam.mx*